Available online at www.sciencedirect.com
SCIENCE DIRECT®
Optics Communications 223 (2003) 91–95
OPTICS COMMUNICATIONS
www.elsevier.com/locate/optcom

Demonstration of narrowband high-reflectivity Bragg gratings in a novel multimode fiber

Y. Sun [a,*], T. Szkopek [b], P.W.E. Smith [a]

[a] Department of Electrical and Computer Engineering, University of Toronto, 10 Kings College Road, Toronto, Ont., Canada M5S 3G4
[b] Electrical Engineering Department, University of California at Los Angeles, 420 Westwood Plaza, Los Angeles, CA 90095-1594, USA

Received 25 November 2002; received in revised form 7 May 2003; accepted 10 June 2003

Abstract

Fiber Bragg gratings are important components for a great number of applications including DWDM lightwave systems, fiber lasers, and sensors. A narrowband high-reflectivity response in a multimode fiber could have a dramatic impact on lightwave communication systems and sensors. In this paper, we report what is, to our knowledge, the first demonstration of strong Bragg reflection gratings in a multimode fiber. Using a novel multimode fiber with standard phase mask writing techniques, we have produced gratings with reflectivities of >98% and bandwidths of <0.5 nm at ~1550 nm in very good agreement with modeling predictions.

PACS: 42.79.Dj; 42.81.–i; 42.79.Sz

Keywords: Fiber Bragg grating; Multimode fiber; Optical fiber communications

1. Introduction

Since Hill and his coworkers [1] first demonstrated the formation of permanent gratings in an optical fiber in 1978, a great deal of worldwide effort has been put into the development of fiber Bragg gratings. At present, Bragg gratings in single mode fibers have been used commercially in optical fiber communications networks and in fiber sensor systems. However, Bragg gratings in multimode fibers have received relatively little attention because of spectral spreading and low reflectivity due to differing modal phase velocities. In 1994, Wanser et al. [2] first calculated the theoretical spectrum of multimode fiber Bragg gratings and suggested their use for sensing microbends. Mizunami et al. [3] experimentally confirmed the spectral properties of multimode fiber Bragg gratings. A grating was fabricated in a graded index (GRIN) fiber with a reflection spectrum 15 nm wide containing multiple peaks and centered at 1560 nm. This group later reported a detailed analysis of multimode fiber Bragg grating behavior [4], including temperature and polarization characteristics. Multimode fibers have the advantage of easy coupling to inexpensive

* Corresponding author. Tel.: +1-416-9780602; fax: +1-416-9713020.
E-mail address: yingzhi.sun@utoronto.ca (Y. Sun).

0030-4018/03/$ - see front matter © 2003 Elsevier Science B.V. All rights reserved.
doi:10.1016/S0030-4018(03)01636-5

light sources, such as light-emitting diodes (LEDs). In particular, GRIN multimode fibers have relatively low-modal group velocity dispersion. These two factors, in conjunction, have led to the predominant use of GRIN multimode fibers in local area network (LAN) applications. However, the characteristics of wide bandwidth and low-reflectivity in multimode fiber gratings provide fundamental limitations for their use in local area optical networks and in other areas.

A recent breakthrough is the proposal of a novel fiber structure with modal propagation characteristics tailored to permit the fabrication of narrowband high-reflectivity multimode Bragg fiber gratings [5]. It was shown that under suitable excitation conditions, this fiber design permits modal effective index degeneracy for modes with circular symmetry – which should be the only modes excited with an axially symmetric coherent laser beam. Under these conditions, Bragg gratings should provide a narrowband response with a reflectivity approaching 100%.

In this letter, we report the first experimental demonstration of high-reflectivity gratings in this novel fiber structure. These gratings had spectral responses with widths of <0.5 nm in the vicinity of 1550 nm, and with >16 dB transmission loss on resonance.

2. Fiber Bragg gratings in novel multimode fiber

In the case of step-index multimode fiber, the interaction of a forward propagating mode with a fiber grating will result in significant reflection when the Bragg condition is satisfied as follows:

$$\beta_i = \frac{2\pi}{\Lambda} + \beta_r, \tag{1}$$

where β_i and β_r are the incident and reflected light longitudinal propagation constants, respectively, and Λ is the period of the gratings. If the incident mth mode couples to same mth mode in the counter-propagating direction, we have $\beta_i = -\beta_r$. The resonant condition for mode m is

$$\lambda_i = 2n_m\Lambda \tag{2}$$

where λ_i is the incident vacuum wavelength and n_m is the effective index of the mth mode. Thus, each mode in a multimode fiber grating will experience resonance at a different vacuum wavelength. As a consequence, there is a limit on the bandwidth narrowness that can be achieved by a multimode fiber grating (MMFG) which is proportional to the maximum spread in effective index for the various modes supported in the fiber. The spread in resonant wavelengths also results in the low-peak reflectivity observed in MMFGs written in standard GRIN fiber [2].

Our novel multimode fiber structure consists of alternating cylindrical shells of higher and lower-refractive index material, as depicted in Fig. 1. This structure is intended to minimize the difference in propagation constants of the various guided modes. To develop an intuitive understanding for the design of a multimode fiber (MMF) that will minimize the difference in propagation constants, we consider an analogy between the propagation of an electromagnetic mode within a fiber and a bound quantum mechanical particle in a potential well. In the scalar approximation for the electromagnetic mode field, the fiber problem can be described by a Schrödinger equation similar to that for a bound particle:

$$[\nabla_T^2 + k_0^2(n^2(r) - n_{eff}^2)]\Psi(r) = 0, \tag{3}$$

where ∇_T is the del operator for transverse spatial co-ordinates, r is the radial position coordinate, k_0 is the vacuum wave vector, $n(r)$ is the radial index profile, n_{eff} is the effective index, and $\Psi(r)$ is the scalar field. The energy eigenvalues of a bound particle are analogous to the effective indices of the modes in the fiber. If a quantum well is made sufficiently shallow, it will contain one energy level, which would be analogous to a single mode

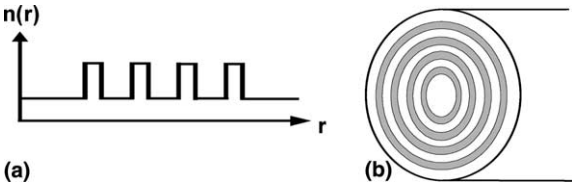

Fig. 1. (a) Refractive index profile. (b) Fiber side view. Shaded regions represent areas of higher-refractive index and unshaded regions represent uniform cladding regions with lower-refractive index.

fiber. The situation of interest is that of closely spaced potential wells. As the wells are brought closer together, the energy level splitting increases. The analogous result then implies that a fiber with periodically varying radial index profile as shown in Fig. 1 should have many modes with very closely spaced effective indexes or propagation constants, which would enable a narrowband reflection response while still supporting multiple modes. By minimizing the difference in propagation constants, all modes in this novel multimode fiber will interact with Bragg gratings in approximately the same way. This allows a reflection response in the novel multimode fiber that is very similar to that in a standard single mode fiber. The close spacing of the effective indexes for different modes is exactly what is needed for the design of narrowband MMFGs.

In the special case in which the thickness of the cylindrical shell (parts of higher-reflective index) is small compared to its mean radius, the shell approximates a planar structure. Thus, the condition for single-mode (ignoring polarization for the moment) operation in each isolated cylindrical shell can be appreciated using simple planar waveguide analysis.

The restriction on the normalized parameter V, here defined for an individual shell is

$$V \equiv \frac{2\pi t\sqrt{n_{\text{shell}}^2 - n_{\text{cladding}}^2}}{\lambda} < \pi \tag{4}$$

for a TE mode, where n_{shell} and n_{cladding} are the shell and cladding refractive indexes, t is the shell thickness and λ is the vacuum wavelength. However, there still exist modes with angular wave vector components, and decreasing the index difference cannot eliminate these modes.

We have recently published simulations for a novel MMF structure with four shells of fixed width, but varying position [5]. The normalized frequency V used was 3.0807, corresponding to $n_{\text{shell}} = 1.505$, $n_{\text{cladding}} = 1.500$, and $t = 4\lambda$. The radius of the innermost shell was varied from 10λ to 30λ, while the shell separation was independently varied from 3λ to 15λ.

The normalized propagation constant b is defined by

$$b = \frac{n_{\text{eff}}^2 - n_{\text{cladding}}^2}{n_{\text{shell}}^2 - n_{\text{cladding}}^2}, \tag{5}$$

where n_{eff} is the effective index of a particular mode. From a study of the maximum spread in the b parameter for modes with harmonic parameter $p = 1$, two significant trends were apparent. The spread in the b parameter ceases to significantly decrease as the shell separation is increased beyond 10λ. Thus, we conclude that for our fiber design, the shell separation need not be greater than 10λ. The second significant trend was the decrease in the spread of the b parameter as the inner shell radius increases. As little decrease was seen beyond an inner shell radius of 25λ, this was the value we used for our fiber design.

The dependence of b upon the p parameter for the proposed MMF structure was also investigated. Simulation results for an MMF structure with four shells of thickness of 4λ, first shell radius of 25λ, shell spacing 10λ, and $V = 3.0807$ are presented in Fig. 2. A total of 240 modes (not including the multiplicity associated with $\pi/2$ rotations for HE and EH modes) were solved with p ranging from 0 to 43. For values of p below four, the b parameters are concentrated about the value 0.64. As p increases for the simulated MMF, the b

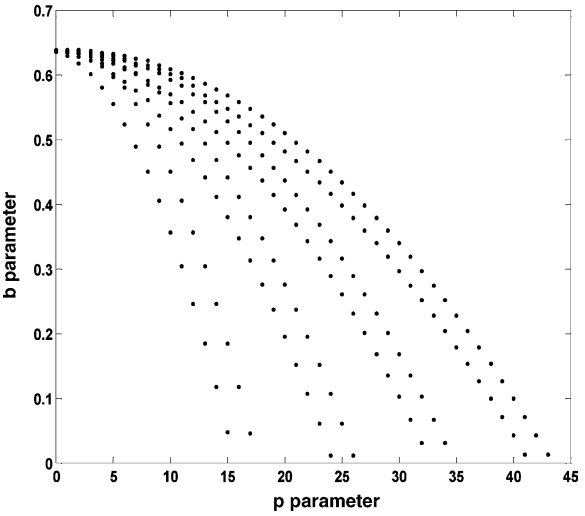

Fig. 2. Numerical simulation results for the b parameter as a function of the p parameter. The concentric shell MMF was simulated with shell thickness = 4λ, first shell radius = 25λ, shell spacing = 10λ, and $V = 3.0807$ from [5].

values "split" into four pairs, corresponding to two polarization modes localized to each of four rings.

3. Experimental results

A fiber preform was made with four higher-refractive-index shells and pulled into fibers with optimized dimensions suggested by our previous modeling results. These dimensions (first shell radius 25λ; shell thickness 4λ; and shell spacing 10λ) were shown to provide excellent Bragg grating performance when circularly symmetric light is coupled into the fibre. The refractive indices of the shells and cladding for our test fiber are 1.4501 and 1.4446, respectively, at $\lambda = 1554$ nm. The increased index in the shells of the fiber was created by GeO_2 doping. This dopant also increases the sensitivity of the fused quartz to the UV light used for writing the Bragg gratings, and thus we expect gratings to be written primarily into the high-index shells. Initial tests of the special fibers were made by coupling light into the fiber and analysing the output with a video camera. The coupling of light into the novel fiber was tested by observing the transmitted light through a 1.63-m segment of fiber at the exit face. When the entire entrance face was uniformly illuminated, the transmitted light was observed to be tightly confined in the high-index shell regions. For broadband "white light" excitation, the output rings had no visible structure, while for narrowband (He–Ne laser or Er fiber amplifier ASE) excitation, some angular intensity variations were observed. In all cases the output light was observed to maintain the polarization of the input.

We wrote Bragg gratings in these fibers using standard phase mask techniques. The fibers were pre-soaked with H_2 gas at 1900 psi for 30 days at room temperature to increase the UV photosensitivity. We wrote the gratings using a 2.5-cm long uniform phase mask designed for writing gratings at 1550 nm with a nulled zeroth-order diffraction peak. The fiber was exposed to 248 nm pulses with an energy of 18 mJ for a total duration of 13 min using a KrF excimer laser operating at a repetition rate of 40 Hz. The gratings in the multimode fiber were interrogated with an Er-fiber amplified spontaneous emission (ASE) light source. An optical spectrum analyzer (Ando AQ 6317B) was used to measure the spectrum of the light transmitted through the fiber gratings. The deepest transmission nulls were obtained with the smallest diameter fiber (32 μm inner-shell diameter, 128 μm cladding diameter). High-reflectivity Bragg fiber gratings centered at 1554 nm were written in the novel multimode fiber as evidenced by the spectra shown in Fig. 3. The transmission loss at the 1554-nm center wavelength is greater than 16 dB. This corresponds to a grating reflectivity of approximately 98%. The bandwidth of the grating response is <0.5 nm at the 3 dB point.

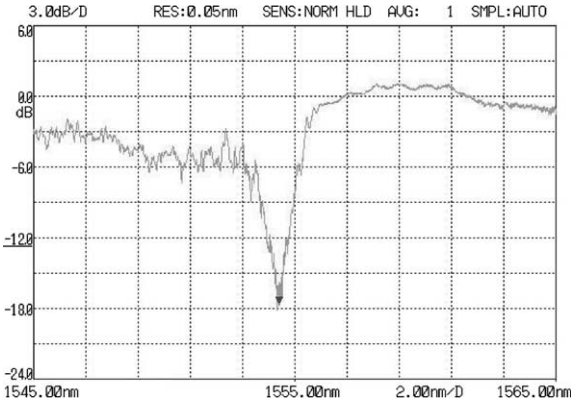

Fig. 3. Transmission spectrum of a Bragg grating written in the novel multimode fiber by the use of a uniform phase mask and measured using an Er fiber ASE light source.

4. Discussion

In a previous publication [5], we presented a theoretical simulation of Bragg grating performance in this novel multimode fiber. Under conditions where only modes of circular symmetry are excited, we can expect to be able to achieve peak reflectivities of 100% with full-width at half-maximum (FWHM) bandwidth of $2.5 \times 10^{-4}\lambda$ which is $\sim$0.4 nm for a Bragg grating wavelength of 1554 nm. In this regime, the bandwidth is determined by the intrinsic width of the grating resonance associated with each nearly degenerate fiber mode excited. In our experiments, we observed a

transmission dip corresponding to a reflectivity of ~98% with a 3 dB bandwidth of <0.5 nm. The conditions for our experiments were somewhat different from those assumed in the theoretical simulations, but we believe that the close agreement with the simulations indicates that the multimode fiber grating is basically performing as expected.

To determine the effective index of the modes that contributed to the transmission spectrum of Fig. 3, we used the same phase mask that we had previously used for the novel multimode fiber to write gratings in a single-mode fiber (Corning SMF-28) for which the fiber parameters are well characterized. The effective index for the modes excited in the novel multimode fiber could then be calculated from a comparison of the wavelength of the grating resonance in the SMF-28 fiber with the wavelength for the grating resonance in a large-diameter novel multimode fiber for which the conditions of our modeling analysis in [5] apply (first shell radius 25λ; shell thickness 4λ; and shell spacing 10λ). We found that the effective index corresponds to a normalized propagation constant $b = 0.64$, in very good agreement with the calculated constant b for the low-order near-degenerate modes (see Fig. 2). This is consistent with our analysis of coupling into modes of the novel fiber that indicates that coherent light couples primarily into low p modes of circular symmetry [7].

The spectra in Fig. 3 show a significant (~2 dB) loss on the short wavelength side of the Bragg resonance. This is somewhat larger than the ~1 dB radiation loss usually seen with single mode fiber gratings [6]. We speculate this larger radiation loss is due to the asymmetric nature of the Bragg grating written with lateral UV exposure. The substantial path difference between one side of the outer shell and the other results in a blazed grating being written, and one would expect the asymmetry to cause mode mixing and thus produce a broad reflection pedestal. A symmetrical exposure technique would likely improve the grating performance, and permit larger-diameter fibers to be used.

5. Conclusions

We have successfully realized the goal of enabling narrowband high-reflectivity gratings to be written in a novel multimode fibre structure consisting of alternating high- and low-refractive index shells. We believe that multimode fibre Bragg gratings will provide another option to the local area network designer, and also influence the development of fiber optic probes in biomedical applications.

Acknowledgements

The authors thank Photonics Research Ontario for providing us with the equipment used for writing fiber Bragg gratings, and for funding support. Additional support for this project was provided by the Natural Sciences and Engineering Research Council of Canada.

References

[1] K.O. Hill, Y. Fujii, D.C. Johnson, B.S. Kwawasaki, Appl. Phys. Lett. 32 (1978) 647.
[2] K.H. Wanser, K.F. Voss, A.D. Kersey, Proc. SPIE 2360 (1994) 256.
[3] T. Mizunami, S. Gupta, T. Yamao, T. Shimomura, in: International Conference on Integrated Optics Optical Fiber Commun./European Conference on Optical Communication, vol. 3, 1997, p. 182.
[4] T. Mizunami, T.V. Djambova, T. Niiho, S. Gupta, J. Lightwave Technol. 18 (2000) 230.
[5] T. Szkopek, V. Pasupathy, J.E. Sipe, P.W.E. Smith, IEEE J. Selected Topics in Quantum Electron. 7 (2001) 425.
[6] V. Mizrahi, J.E. Sipe, J. Lightwave Technol. 11 (1996) 1513.
[7] V. Pasupathy, Novel multimode fibre gratings for medical Raman spectroscopy M.Sc. Thesis, University of Toronto, 2001.